SCALING OF BASIN-SIZED IMPACTS AND IMPLICATIONS FOR THE MOON AND EARLY EARTH

Ross W. K. Potter[1,2,3], David A. Kring[2,3] and Gareth S. Collins[4], [1]Dept. Earth, Environmental and Planetary Sciences, Brown University, Providence, RI, 02912, USA, [2]Center for Lunar Science and Exploration, Lunar and Planetary Institute, 3600 Bay Area Boulevard, Houston, TX, 77058, USA, [3]NASA Solar System Exploration Research Virtual Institute, ross_potter@brown.edu; [4]Dept. Earth Science and Engineering, Imperial College London, SW7 2AZ, UK.

Introduction: Impact cratering is a fundamental geologic process that occurs over a truly vast scale – from sub-millimeter micro-craters to thousands-of-kilometer basins. Knowledge of the cratering process, however, diminishes as scale increases. Consequently, the largest class of impact structure, basins, is the least understood. Impact experiments [1-3] have provided valuable information on the cratering process, but cannot fully replicate all aspects of basin-scale impact events (e.g., melt production). Basin-scale impact events can also be investigated through numerical modeling. The majority of basin-scale impact modeling has addressed lunar basins due to their prevalence and preservation, which has provided an opportunity to measure properties (e.g., with the GRAIL and LRO spacecraft) that can be used to constrain the models. Here, data output from a suite of recent lunar basin numerical models [4-7] has been further interrogated to formulate a set of scaling laws specifically for basin-scale impacts.

Methods: The iSALE shock physics code [e.g., 8] was used to model basin-forming events on the Moon. The models approximated the thermodynamic and compressible nature of lunar materials by using a Tillotson equation of state for gabbroic anorthosite [5,9] and a semi-analytical equation of state (ANEOS) for dunite [10] for the crust and mantle, respectively. Dunite was also used to represent the impactor's response to thermodynamic and compressibility changes. Crustal and mantle strength and thermal properties were calculated from experiments on gabbro [11-13], dunite [13,14] and peridotite [12,15]. Based on GRAIL data [16], crustal thicknesses of 40 and 60 km were used. Target thermal gradients, influenced by lunar thermal evolution models [17], ranged between 10 and 50 K/km to represent the lunar basin-forming epoch (~4.3 to 3.8 Ga).

Cell size varied between 1 and 5 km. Impactors varied from 20 to 250 km in diameter. Impact velocities were between 10 and 20 km/s. The gravity field was a constant 1.62 m/s^2. The 2D version of iSALE was used; consequently all impacts were vertical. This setup should, however, provide the correct azimuthally averaged behavior for the impact process.

Results and discussion:

Basin formation. Figure 1 illustrates lunar basin structure after the dynamic formation phase has ceased (~2 hours after initial impact) for the same (size and velocity) impactor into two targets with different thermal properties. As can be seen, initial target conditions greatly influence the final size and structure of a basin, including the basin rim (r_f) and the annulus of thickened crust (r_{ca}) [5]. The excavation phase of basin formation was, however, essentially unaffected by different thermal profiles; transient crater diameters differed by <10% and the excavation depth to diameter ratio was consistently 0.12±0.01, agreeing with the vast majority of analytical, experimental, geological, and geophysical crater studies. The transient crater formation times were comparable to previous estimates [18]. Scaled excavation depths (excavation depth divided by impactor radius) also matched well with Π-scaling relationships derived from first principles and experimental data [19].

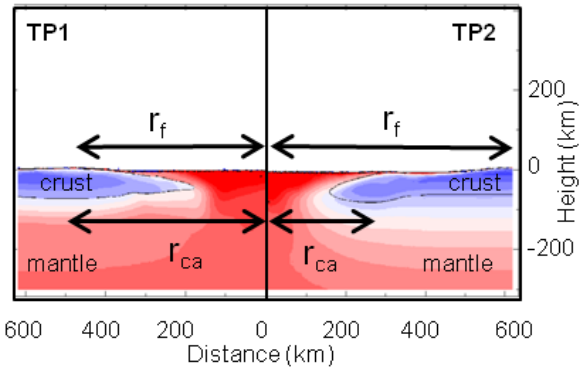

Figure 1: Final basin form for two impacts with the same energy (80 km diameter impactor, 15 km/s velocity) into targets with different thermal profiles (TP). TP1 and TP2 both have a crustal thermal gradient of 10 K/km. In the mantle, temperatures are initially at the solidus in TP1, but are sub-solidus in TP2. r_f is final basin rim radius, r_{ca} is crustal annulus radius.

Melt volume. Melt volumes for the lunar basin-scale impacts (10^6-10^7 km^3) were comparable to scaling relationships [20] and other numerical models [21] that also take into account thermal gradients.

Basin size. The basin rim was defined here as the radial distance from the basin center to the highest topographic point. For a thermal gradient of 10 K/km the transient crater was ~0.40 of the final crater rim. Terrestrial crater studies suggest a transient crater of

0.5-0.65 that of the final crater (radius) [22]. Severe modification of the transient cavity, due to the relatively warm (weak) target and the size of basin-scale impactors, explains why the final crater is relatively larger compared to the dimensions of the transient crater.

The Moon. The transient crater is particularly useful for determining impact kinetic energy and the impactor size. In the field or in planetary surface images, however, the observable feature is the final basin diameter. In Figure 2, we provide a method for determining impactor radius directly from the final crater radius. The crater rim radius is plotted against impactor radius for a number of the lunar basin-forming impacts. Unsurprisingly, larger and faster impactors produce larger basins. Impacts at 15 km/s into thermal profiles (TP) 1 and TP2 (and TP3) suggest that lunar basins up to Imbrium in size (crater rim radius ~600 km) were produced by impactors 10-50 km in radius. This is consistent with impactor sizes derived from lunar crater size-frequency distributions [23].

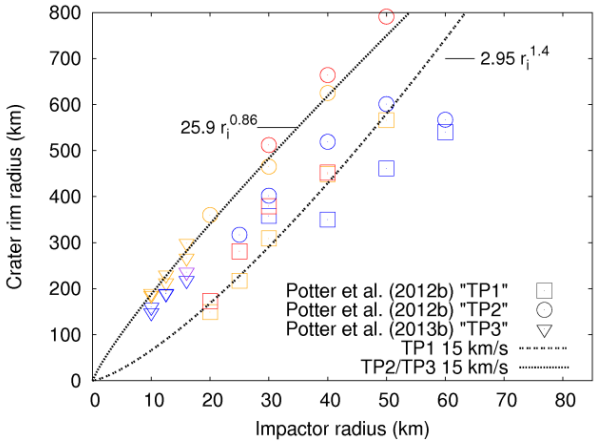

Figure 2: Crater rim radius against impactor radius (r_i) for a suite of lunar basin-forming impacts. Blue symbols represent impacts at 10 km/s; orange symbols, 15 km/s; red symbols, 20 km/s. Fits to impacts at 15 km/s are shown.

Early Earth. The results of this work can also be applied to basin-forming events on other silicate planetary bodies prior to 3.8 Ga, such as Earth. Our thermal gradient estimates are comparable to lower end estimates for the Hadean Earth (12 K/km [24]) and, therefore, imply that basin-forming impacts on the early Earth would also follow proportional scaling, be heavily affected in the modification phase by the pre-impact thermal conditions, and create comparable volumes of melt. Based on this scaling, material in the largest Hadean impacts would have excavated material from depths >200 km, though melting would have been much deeper [25] suggesting mainly mantle-derived melt compositions. Impacts may have generated subsurface hydrothermal subsystems that persisted for hundreds of thousands to millions of years [e.g., 26]. Scaling laws here imply longer lived hydrothermal systems, geographically larger systems, or a combination of both.

Conclusions: Numerical modeling has shown many aspects of basin-scale impacts are consistent with Π-scaling relationships, and the vast majority of analytical, experimental, geological and geophysical studies. The models demonstrate that target conditions do not affect basin excavation, but greatly affect basin modification, manifesting in a transient crater which is ~40% of the final crater rim when the (lunar) crust was as warm as it was >3.8 Ga.

Acknowledgements: We thank the iSALE developers: Boris Ivanov, Jay Melosh, Kai Wünnemann and Dirk Elbeshausen. This work was supported by SSERVI.

References: [1] Gault, D. E. and Wedekind, J. A. (1978) *Proc. 9th LPSC*, 3843-3875. [2] Burchell, M. J. and Mackay, N. G. (1998) *JGR*, 103, 22761-22774. [3] Housen, K. R. and Holsapple, K. A. (2003) *Icarus*, 163, 102-119. [4] Potter, R. W. K. et al. (2012) *Icarus*, 220, 730-743 [5] Potter, R. W. K. et al. (2012) *GRL*, 39, L18203 [6] Potter, R. W. K. et al. (2013) *JGR*, 118, 963-979. [7] Potter, R. W. K. et al. (2013) *GRL*, 40, 5615-5620. [8] Collins, G. S. et al. (2004) *MAPS*, 39, 217-231. [9] Ahrens, T. J. and O'Keefe, J. D. (1977) In: *Impact and explosion cratering*, Pergamon, New York, 639-656. [10] Benz, W. et al. (1989) *Icarus*, 81, 113-131. [11] Azmon, E. (1967) NSL 67-224. [12] Stesky, R. M. et al. (1974) *Tectonophys.*, 23, 177-203. [13] Shimada, M. et al. (1983) *Tectonophys.*, 96, 159-192. [14] Ismail, I. A. H. and Murrell, S. A. F. (1990) *Tectonophys.*, 175, 237-248. [15] McKenzie, D. and Bickle, M. (1988) *J. Petrol.*, 29, 625-679. [16] Wieczorek, M. A. et al. (2013) *Science*, 339, 671-675. [17] Spohn, T. et al. (2001) *Icarus*, 149, 54-65. [18] Melosh, H. J. and Ivanov, B. A. (1999) *Ann. Rev. Earth. Planet. Sci.*, 27, 385-415. [19] Holsapple, K. A. (1993) *Ann. Rev. Earth Planet. Sci.*, 21, 333-373. [20] Abramov, O. et al. (2012) *Icarus*, 218, 906-916. [21] Marinova, M. M. et al. (2011) *Icarus*, 211, 960-985. [22] Grieve, R. A. F. et al. (1981) In: *Multi-ring Basins*, Pergamon, New York, 37-57. [23] Strom, R. G. et al. (2005) *Science*, 309, 1847-1850. [24] Hopkins, M. D. et al. (2010) *EPSL*, 298, 367-376. [25] Cintala, M. J. and Grieve, R. A. F. (1998) *MAPS*, 33, 889-912. [26] Kring, D. A. (2003) *Astrobiology*, 3, 133-152.